THE UNIVERSITY *of* EDINBURGH

Edinburgh Research Explorer

The presence of valine at residue 129 in human prion protein accelerates amyloid formation

Link:
[Link to publication record in Edinburgh Research Explorer](#)

Document Version:
Publisher's PDF, also known as Version of record

Published In:
FEBS Letters

OPEN ACCESS

The presence of valine at residue 129 in human prion protein accelerates amyloid formation

Ilia Baskakov[a], Petra Disterer[b], Leonid Breydo[a], Michael Shaw[b], Andrew Gill[c], William James[b], Abdessamad Tahiri-Alaoui[b,*]

[a] *Medical Biotechnology Center, University of Maryland Biotechnology Institute, Baltimore, MD 21201, USA*
[b] *Sir William Dunn School of Pathology, University of Oxford, South Parks Road, Oxford, OX1 3RE, UK*
[c] *Institute for Animal Health, Compton, Berkshire, Newbury, RG20 7NN, UK*

Abstract The polymorphism at residue 129 of the human *PRNP* gene modulates disease susceptibility and the clinicopathological phenotypes in human transmissible spongiform encephalopathies. The molecular mechanisms by which the effect of this polymorphism are mediated remain unclear. It has been shown that the folding, dynamics and stability of the physiological, α-helix-rich form of recombinant PrP are not affected by codon 129 polymorphism. Consistent with this, we have recently shown that the kinetics of amyloid formation do not differ between protein containing methionine at codon 129 and valine at codon 129 when the reaction is initiated from the α-monomeric PrP^C-like state. In contrast, we have shown that the misfolding pathway leading to the formation of β-sheet-rich, soluble oligomer was favoured by the presence of methionine, compared with valine, at position 129. In the present work, we examine the effect of this polymorphism on the kinetics of an alternative misfolding pathway, that of amyloid formation using partially folded PrP allelomorphs. We show that the valine 129 allelomorph forms amyloids with a considerably shorter lag phase than the methionine 129 allelomorph both under spontaneous conditions and when seeded with pre-formed amyloid fibres. Taken together, our studies demonstrate that the effect of the codon 129 polymorphism depends on the specific misfolding pathway and on the initial conformation of the protein. The inverse propensities of the two allelomorphs to misfold in vitro through the alternative oligomeric and amyloidogenic pathways could explain some aspects of prion diseases linked to this polymorphism such as age at onset and disease incubation time.
© 2005 Federation of European Biochemical Societies. Published by Elsevier B.V. All rights reserved.

Keywords: Prions; Polymorphism; Codon 129; Amyloid; Folding

1. Introduction

The human PrP gene (*PRNP*) has two common allelic forms that encode either methionine or valine at codon 129. This polymorphism is a key determinant of susceptibility to sporadic [1] and acquired [2,3] prion diseases, and may affect age at onset [4–6]. An understanding of the role of this poly-morphism as a powerful genetic modifier may provide clues as to the molecular mechanisms that mediate prion propagation. One approach is to study the folding of the two allelic variants of recombinant human PrP in vitro. Four major routes of folding denatured, disulphide-oxidized PrP in vitro have been described [7–10] (see Fig. 1). The first, which is extremely rapid under near-neutral, non-denaturing conditions, produces an α-helix-rich, soluble, monomeric form that is believed to resemble the physiological form. It has been shown that the thermodynamic stability of this form is not affected by the codon 129 polymorphism [11]. NMR structure analysis has been used to investigate the structural basis of inherited human transmissible spongiform encephalopathies and showed that only part of the disease-related amino acid replacements lead to reduced stability of the cellular form of PrP [12]. Recently, the three-dimensional structure of the monomeric, Val129 form of human PrP was determined [13], from which it was concluded that the polymorphism at codon 129 has no measurable effect on the folding, dynamics and stability of normal cellular PrP. The second major route of folding, favoured at low pH under moderately denaturing conditions and high PrP concentrations, results in the formation of a soluble, oligomeric form that shows significant resistance to proteinase K and matures over time to become dominated by β-sheets [8,9]. We have recently shown that the kinetics of the β-oligomer formation is affected by the residue encoded at position 129. We showed that Met129 has a higher propensity to oligomerize than Val129 and that the further maturation of the oligomers was more rapid for the Met129 variant than the Val129 variant [9].

The third major pathway of in vitro folding produces high molecular weight multimers that aggregate to form amyloid fibres and is favoured under moderately denaturing conditions, neutral pH and with agitation [8,14]. This form is partially sensitive to proteinase K digestion. Significantly, it has been reported, recently, that the amyloids generated through this third pathway from recombinant mouse PrP were infectious and produces transmissible disease when inoculated into transgenic mice [15]. This result is a major milestone in that it appears to confirm the "protein only" hypothesis in mammalian prion diseases [15,16]. It also suggests that the amyloids form of recombinant PrP and/or other misfolded intermediates may represent the infectious entity in TSE diseases. Recently, we have found that the polymorphism at codon 129 has no measurable effect on the amyloid

*Corresponding author. Fax: +44 1865 285756.
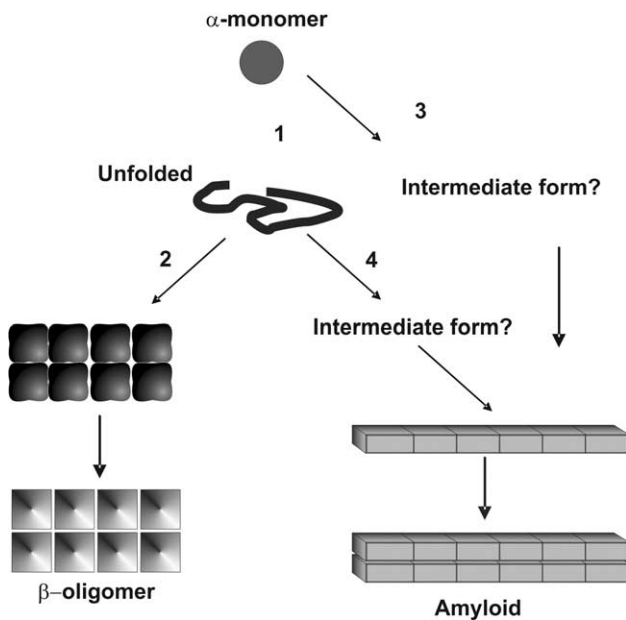*E-mail address:* abdou.tahiri-alaoui@path.ox.ac.uk (A. Tahiri-Alaoui).

Fig. 1. Model of the multiple folding pathways of recombinant human PrP in vitro (adapted from Tahiri-Alaoui and James [10]). Various routes of folding of recombinant, disulphide-oxidized PrP have been discussed in the literature (Baskakov et al. [7,8]): pathway 1, from the denatured state to α-helical monomeric state; pathway 2, from the denatured state to PK-resistant oligomeric form [9]; pathway 3, from α-helical monomeric state to amyloid form [10]; pathway 4, from partially unfolded state to multimeric aggregate and hence to amyloid form. The present work describes the misfolding of recombinant human PrP[90–231] through pathway 4 in the context of the polymorphism at codon 129.

accumulation when the reaction is initiated from the α-helical monomeric form [10] (see pathway 3 in Fig. 1). This is in contrast to the substantial effect that this common polymorphism can exert on the formation of soluble β-oligomer when the misfolding is initiated from denatured state (see pathway 2 in Fig. 1) [9]. This suggests that the conformational transitions, in which residues at position 129 contribute to significant free energy changes, are likely to be confined to more disordered states than those shared by the α-monomers of the PrP [10]. In order to test this, we decided to analyse the effect of the polymorphism at codon 129 on the pathway four as depicted in Fig. 1, by initiating the amyloid formation from a partially folded state and that is under both spontaneous and seeded conditions. The rational behind this is to allow the two allelomorphs to explore freely the misfolding landscape permitted under amyloid forming conditions.

2. Materials and methods

2.1. Preparation of recombinant human prion protein allelomorphs

The recombinant human PrP[90–231] proteins were prepared and purified as previously described [9]. Briefly, the genomic DNA encoding methionine/valine at codon 129 of PRNP gene was extracted from the blood of a heterozygote individual using standard phenol–chloroform methods. The fragment of the PRNP gene spanning codon 90 through 231 was amplified and cloned into the pTrcHis2B vector that incorporated a C-terminal His-tag (Invitrogen life technologies, Paisley, UK) according to the manufacturer's instructions. The identity of human PrP clones was confirmed by sequencing with the BigDye Terminator v3.0 on ABI-Prism 3100 Genetic Analyzer (Applied Biosystems). The clones corresponding to PrP[90–231] with Met129 or

Val129 were identified by comparison with human PrP clones available in the databases (Accession Nos.: M13667, P04156). The expression of both recombinant PrP variants was done in Escherichia coli and the purification was performed as previously described [9]. Stocks of highly purified proteins were stored in 6 M guanidine hydrochloride containing 50 mM Tris–HCl, pH 7.2.

2.2. Amyloid reactions, thioflavin T assay and kinetic analysis

Time course study of amyloid formation of recombinant human PrP[90–231] was carried out as previously described [8] by monitoring thioflavin T (ThT) fluorescence. Briefly, proteins in 6 M guanidine hydrochloride were diluted to a final concentration of 35 μM in phosphate buffered saline, pH 7.2, containing 3 M urea, 0.02% azide and a final concentration of 1 M guanidine hydrochloride. Samples were incubated at 37 °C under continuous shaking at 600 rpm on a Delfia plate shaker in 1.5 ml Eppendorf tubes. To mimic the situation in heterozygote individuals, methionine 129 and valine 129 variants were mixed at 1:1 molar ratio. The final protein concentration was kept at 35 μM. In the homologous and heterologous seeding experiments, an aliquot of preformed fibrils was taken from the stationary phase and considered to contain 100% seeds, this was then used to inoculate freshly prepared amyloid reaction at a final seed concentration of 1%.

The kinetics of amyloid formation were analysed by fitting time-dependent changes in ThT fluorescence of samples to the following sigmoidal equation using non-linear, least squares analysis (GraphPad Prism vs. 4.01).

$$F_{ThT} = A/(1 + e^{(-B(t-t_i))}), \tag{1}$$

where F_{ThT} is the fluorescence intensity of ThT, A is the ThT fluorescence intensity in the post-transition plateau, t_i is the inflection point, i.e., the midpoint of the transition region, B (h^{-1}) is the amyloid growth rate constant, and t is the time in hour. The lag time (t_{lag}) of amyloid formation was calculated by extrapolation of the linear region of the sigmoidal transition phase of ThT fluorescence to the abscissa intercept [17].

2.3. Size-exclusion high performance liquid chromatography

Rapid refolding of proteins into α-monomeric form was carried out by size-exclusion HPLC as previously described [9] with the following modifications: Proteins, in 100 μl volume at 5 mg/ml from unfolded state in 6 M guanidine hydrochloride, 50 mM Tris–HCl, pH 7.2, were injected onto TSK-Gel SWXL G3000 HPLC column, 7.8 × 300 mm (Phenomenex, Macclesfield, UK), equilibrated in 50 mM sodium acetate, pH 5.5, 150 mM sodium chloride, 1 M urea and 0.02% azide. The peak corresponding to monomeric proteins was manually collected and the folding of the proteins was assessed by circular dichroism (CD). All HPLC separations were performed at room temperature with a flow rate of 1 ml/min by means of a Perkin–Elmer HPLC system composed of a Binary LC pump 250 and a Diode array detector 235C controlled by Total Chrome software version 6.2 (Perkin–Elmer, Seer Green, UK), through a PE Nelson 600 series link. The eluent was monitored by UV absorption at 280 nm.

2.4. Circular dichroism and Fourier transform infra-red spectroscopy

CD spectra were recorded using a Jasco-720 spectrometer at 37 °C in the amyloid buffer (phosphate buffered saline, pH 7.2, containing 3 M urea, 0.02% azide and a final concentration of 1 M guanidine hydrochloride) at around 35 μM protein concentration using the following parameters: Cell path 0.1 cm, speed 55 nm/s, band width 1.0 nm, resolution 0.5 nm and response 4 s. Four individual scans were averaged and the buffer spectra were subtracted. Fourier transform infra-red spectroscopy (FTIR) spectra were collected by means of a Bruker Tensor 27 FTIR instrument (Bruker Optics, Billerica, MA) equipped with a MCT detector cooled with liquid nitrogen. The amyloids were dialyzed against 10 mM Na-acetate buffer (pH 5.5), 10 μl of each sample was loaded into BioATRcell II, 128 scans at 2 cm^{-1} resolution were collected under constant purging with nitrogen, corrected for water vapours and background spectra of buffer were subtracted.

2.5. Negative staining and transmission electron microscopy

Aliquots of 3 μl were taken from samples containing amyloid fibrils as judged from ThT fluorescence, loaded onto carbon-coated, glow-discharged 400-mesh copper grids, blotted, negatively stained with 1%

uranyl acetate, air dried and then viewed in a Zeiss (formerly Leo) Omega 912 electron microscope equipped with an in column charge-coupled device camera (2048 × 2048 pixels) from Proscan, Germany [18].

3. Results

In order to gain insights into the global conformation of the PrP allelomorphs at time zero of amyloid reaction, i.e., the time when the proteins were diluted from 6 M guanidine hydrochloride into the amyloid buffer (phosphate buffered saline, pH 7.2, containing 1 M guanidine hydrochloride, 3 M urea and 0.02% azide), we performed simultaneous analyses by size exclusion high performance liquid chromatography and CD (Fig. 2 and inset). Aliquots of 100 μl were taken from the amyloid reactions and injected onto a SEC-HPLC column previously equilibrated in the same amyloid buffer. The Met129, Val129 as well as the mixture (1:1) of both variants eluted with equal retention times, i.e., 8.35 min (Fig. 2). However, when the properly folded α-monomeric PrP was diluted into the same amyloid buffer then subjected to the same SEC-HPLC analysis, its retention time increased to 9.05 min (Fig. 2). These differences in the retention times were indicative of conformational/aggregation differences at time zero between the starting material used in pathway 4 as compared to that used previously to investigate pathway 3 (Fig. 1) [10]. The former has a conformation that was most likely to be characterized by a large hydrodynamic volume, indicating a more open structure;

though the presence of dimers in this state could not be ruled out. CD spectra (inset in Fig. 2) of protein samples used to initiate pathway 4 were also different from those used to initiate pathway 3. The CD spectrum of the latter was characteristic of an α-helix-rich conformation as indicated by the two minima at around 210 and 222 nm. By contrast, the CD spectra of the PrP allelomorphs used to initiate the pathway 4 in Fig. 1 were not typical of α-helix-rich proteins (inset in Fig. 2) but were also not indicative of random coil or typical β-sheet-rich conformation. The presence of 1 M guanidine hydrochloride and 3 M urea in the amyloid forming buffer made it difficult to extract spectral information between 190 and 208 nm. However, one can conclude from the CD and SEC data that all the PrP variants used to initiate the amyloid formation in pathway 4 of Fig. 1 had comparable levels of disordered conformation. Therefore, any differences in the kinetics of the misfolding behaviour would be attributed to the effect of the polymorphism at codon 129.

CD analysis (Fig. 3A–C) revealed conformational changes during amyloid formation through pathway 4 (Fig. 1) that occurred starting from around 3 h after initiating the amyloid reactions. The CD spectra of the two individual PrP variants as well as in the 1:1 mixture displayed the same characteristics up to 12 h during the amyloid reaction. There was a loose isodichroic point at around 214 nm concomitant with a significant change of the CD signal around 222 nm, which seemed to indicate a loss of α-helical conformation. This conformational transition appeared to happen similarly between all the PrP
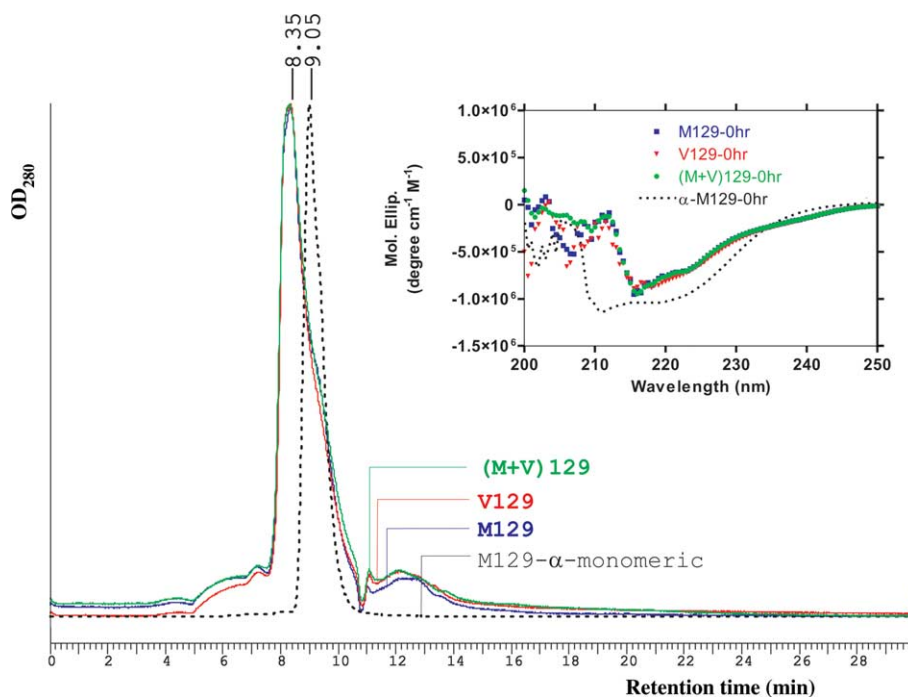

Fig. 2. Chromatographic and spectroscopic characterization of recombinant human PrP$^{90–231}$ allelomorphs. Recombinant human PrP was expressed with either methionine or valine at position 129 in *E. coli*. Proteins were fully oxidized and kept in 6 M guanidine hydrochloride buffered with 50 mM Tris–HCl, pH 7.2. For amyloid reaction through pathway 4 (see Fig. 1), the PrP allelomorphs were diluted into the amyloid buffer (3 M urea, in PBS, pH 7.2, 0.02% azide and the concentration of guanidine hydrochloride adjusted to 1 M), the final protein concentration in the amyloid reaction was 35 μM. Soon after diluting the proteins in the amyloid buffer (time zero), 100 μl was injected onto TSK-Gel SWXL G3000 column previously equilibrated in the same amyloid buffer. As a control, we have used PrP allelomorphs that were previously folded into α-monomeric from Tahiri-Alaoui and James [9] before being diluted into the amyloid buffer. Because both PrP allelomorphs controls and their 1:1 mixture gave super imposable chromatographs only the α-Met129 control is shown in the overlay. The inset shows CD spectra at time zero of amyloid reaction of PrP allelomorphs and the control α-Met129.
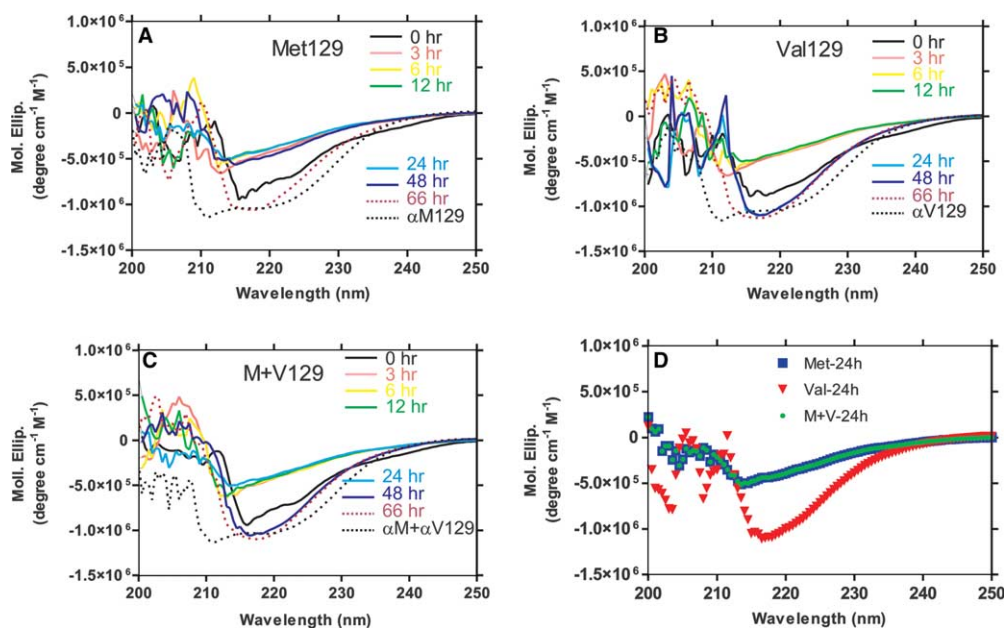
Fig. 3. Circular dichroism spectra of recombinant human PrP[90–231] allelomorphs during amyloid formation. (A), (B) and (C) show overlay of CD spectra of Met129, Val129 and their 1:1 mixture, respectively, during amyloid formation using the conditions described in Fig. 2. For each PrP allelomorph, the spectra of the corresponding alfa-monomeric isoforms acquired at time zero of amyloid reaction are given for comparison to ascertain conformational differences. (D) shows an overlay of CD spectra after 24 h of amyloid reaction to illustrate direct comparison between the PrP allelomorphs and their 1:1 mixture as this is the time point where we see the accelerated acquisition of β-sheet structure that is not seen yet with either M129 or the 1:1 mixture.

variants up to 12 h during amyloid reaction (Fig. 3A–C). However, after 24 h of amyloid reaction, the CD spectrum of the Val129 variant was characteristic of β-sheet rich conformation (Fig. 3D), whilst the Met129 variant and the mixture did not appear to represent a typical β-sheet CD spectra with a single minima at around 218 nm until 66 and 48 h, respectively (Fig. 3A and C).

In order to correlate the changes in conformation seen by CD spectroscopy, especially, the rapid acquisition of β-sheet structure seen in the Val129 variant as compared to the Met129 and the 1:1 mixture, with the kinetics of fibril formation we decide to monitor amyloid formation by ThT assay. A common feature of amyloid structures is their ability to bind dyes such as ThT. The rapid binding of ThT to amyloids is accompanied by a dramatic increase of fluorescence at around 482 nm, when excited at 455 nm. We have used this property to monitor the accumulation of amyloids in vitro at 37 °C (Fig. 4A). The formation of amyloids by both Met129 and Val129 showed a characteristic nucleation-dependent, polymerization pattern, having an initial lag phase followed by a rapid growth phase as measured by ThT fluorescence. The length of the lag phase, however, was significantly different between the two allelomorphs; Met129 had a lag time of 52 h whilst the Val129 allelomorph had a lag time of only 20 h. To mimic the situation of a heterozygote individual carrying both alleles, we analysed amyloid formation in an equimolar mixture of Met129 and Val129 (Fig. 4B). The lag time of amyloid formation in the equimolar mixture was 31.5 h, an intermediate value compared with the unmixed proteins. Notably, in the mixture of Met129 and Val 129 the kinetics of amyloid formation followed a single sigmoidal transition. The amyloid growth rate constant was 0.07 h^{-1} for both alleles individually

and also for the mixture. The total fluorescence of the valine 129 and the methionine 129 variant reached a maximum of around 3000×10^3 and 2500×10^3 counts per second, respectively.

Given the striking difference in the lag times of spontaneous amyloid formation between the two allelomorphs, we hypothesized that the rate of nucleation was the key difference between the two forms. To test this, we examined the effect of pre-formed amyloid seeds on the kinetics of amyloid formation in homologous as well as heterologous reactions (Fig. 5). Seeding the Met129 variant with 1% Met129 amyloid decreased the lag time of fibres accumulation from 52 to 34 h. Similarly, the homologous seeding of the Val129 variant also decreased the lag time of fibres formation from ≈20 to 10 h. Thus, although the lag periods were reduced by similar proportions by seeding in both cases, they were not rendered equal. Seeding with heterologous amyloids had similar effects on lag time as seeding with homologous seeds (Fig. 5B). When the Met129 was seeded with the Val129 the lag time of amyloid accumulation decreased from 52 to 28 h. Similarly, when the Val129 was seeded with the Met129 the lag time of amyloid accumulation decreased from 20 to 14 h.

In contrast to the effect of seeding on lag times, the amyloid growth rate in both homologous seeded reactions remained similar to that of the unseeded reactions. However, seeding with heterologous amyloid revealed that amyloid growth rates were affected by the mismatch in the polymorphic residue at 129 between the seeds and the substrates. Specifically, amyloid growth rate of Met129 dropped from 0.07 to 0.04 h^{-1} when seeded with homologous versus heterologous amyloid seed, respectively, and that of Val129 dropped to 0.05 h^{-1} with heterologous seed. The shorter lag time of amyloid formation of
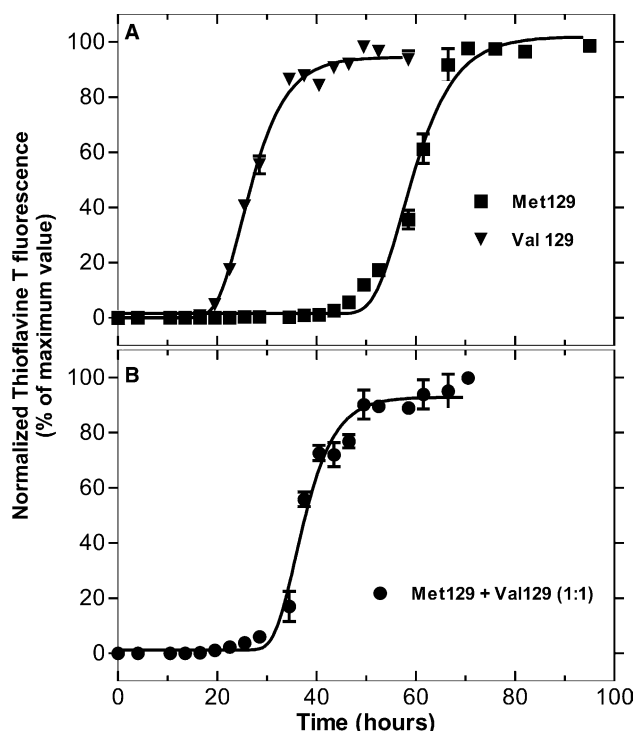
Fig. 4. Effect of the polymorphic residue at position 129 on the kinetics of spontaneous amyloid formation of recombinant human PrP$^{90-231}$ measured by ThT fluorescence. (A) Comparison of the time-dependent change in ThT fluorescence between Met129 (filled squares) and Val129 (filled triangles) allelomorphs. The amyloid reaction was performed at 37 °C under continuous agitation (600 rpm) in 1.5 ml tubes. The proteins were diluted from 6 M guanidine hydrochloride to a final concentration of 35 μM in phosphate buffered saline, pH 7.2, containing 1 M guanidine hydrochloride, 3 M urea and 0.02% azide. (B) represents a time-dependent change in ThT fluorescence during amyloid accumulation in a heterozygote-like reaction that contained 1:1 equimolar mixture of both allelomorphs (filled circle). In (A) and (B), the solid lines represent non-linear, least square fits using the equation described in Section 2.

Fig. 5. Effect of the polymorphic residue at position 129 on the kinetics of seeded amyloid formation of recombinant human PrP$^{90-231}$ measured by ThT fluorescence. (A) Comparison of the time-dependent change in ThT fluorescence between the two PrP allelomorphs during homologous seeding; Met129 in presence of 1% Met129 seed (empty squares) and, Val129 in presence of 1% Val129 seed (empty triangles). (B) Comparison of the time-dependent change in ThT fluorescence between the two PrP allelomorphs during heterologous seeding; Met129 in presence of 1% Val129 seed (empty squares) and, Val129 in presence of 1% Met129 seed (empty triangles). The amyloid reaction was performed at 37 °C under continuous agitation. The proteins were diluted from 6 M guanidine hydrochloride to a final concentration of 35 μM in phosphate buffered saline, pH 7.2, containing 1 M guanidine hydrochloride, 3 M urea, 0.02% azide and 1% of the corresponding amyloid seed. In (A) and (B), the solid lines represent non-linear, least square fits to the data using Eq. (1) described in Section 2.

Val129 versus Met129 was maintained during the homologous and the heterologous seeding.

Amyloid fibres formed under the various experimental conditions showed typical characteristics of amyloids based on transmission electron microscopy (Fig. 6A–C) and FTIR spectroscopy (Fig. 6D). Amyloids from both allelomorphs consist of linear, occasionally twisted, unbranched structures (Fig. 6A–C). Based on transmission electron microscopy, the fibres from both PrP allelomorphs formed under spontaneous or seeded conditions were morphologically indistinguishable. As judged from FTIR, the amyloid fibres produced from both allelomorphs were also conformationally indistinguishable (Fig. 6D). The FTIR spectra of these fibres showed a major band at 1622 cm^{-1} and a minor broad band centred at 1535 cm^{-1}, both are characteristic of β-sheet structures with intermolecular hydrogen bonds. A smaller band at 1693 cm^{-1} was indicative of antiparallel β-sheets and a minor band at 1651 cm^{-1} was a characteristic of α-helices. Furthermore, we have used limited proteinase K digestion combined with electrospray ionization mass spectrometry to compare the amyloid fibres from both allelomorphs (data not shown). Consistent with our previous findings, we found that the fibres
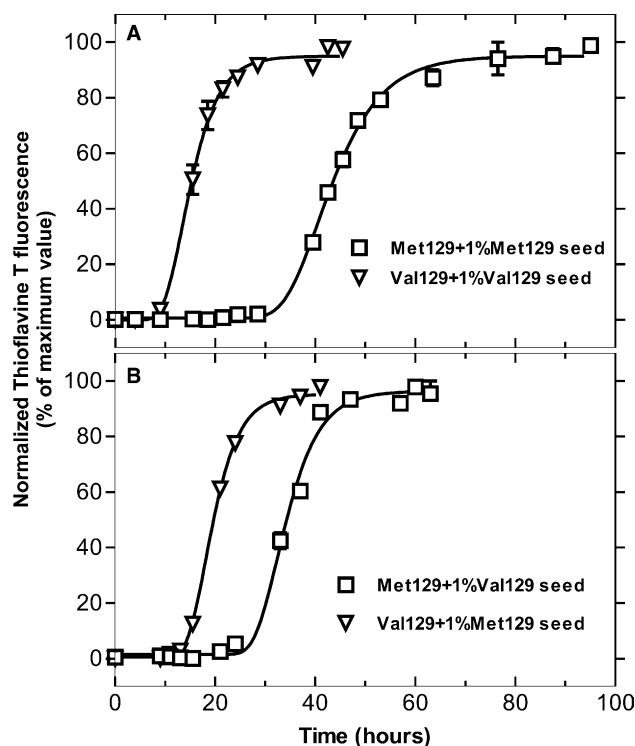
from both PrP variants displayed short PK-resistant core [19,20].

4. Discussion

The present results demonstrate the importance of the polymorphism at codon 129 in modulating the formation of an alternative misfolded form of PrP by allowing the partially folded PrP (pathway 4, Fig. 1) to explore the pathway that leads to amyloid formation. We have found clear differences in the kinetics of amyloid formation between the two allelomorphs. The Val129 variant had a significantly shorter lag time prior to amyloid formation than did the Met129 variant and this correlated well with the rapid acquisition of β-sheet rich conformation by the Val129 allelomorph as compared with the Met129 allelomorph and the 1:1 mixture. These data do not contradict the observation made during the misfolding of α-monomeric PrP into amyloids (pathway 3, Fig. 1), where we have found no measurable effects of the polymorphism at
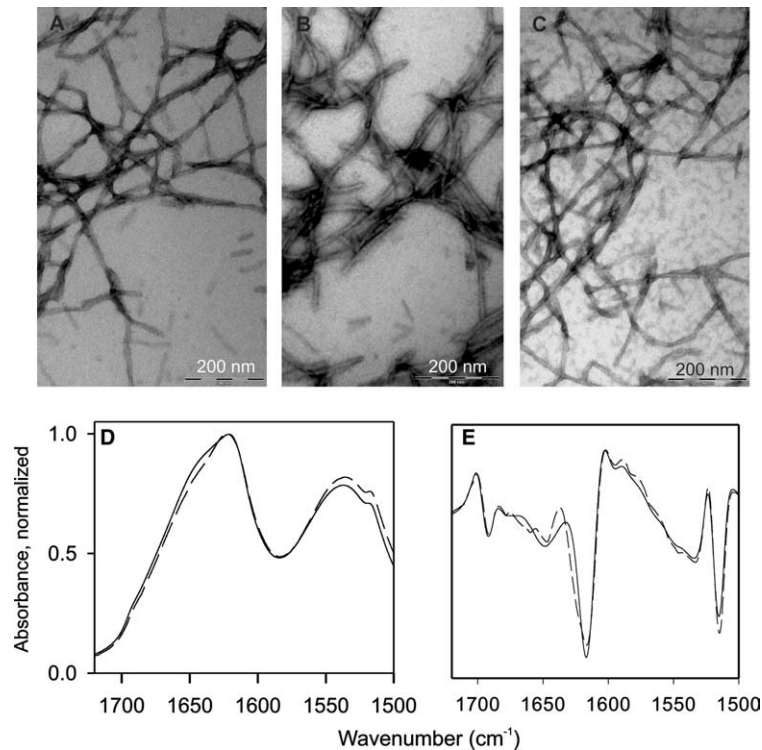
Fig. 6. Transmission electron micrographs and FTIR spectra of amyloids produced from recombinant human PrP[90–231] allelomorphs. (A) is representative micrograph of Met129 variant. (B) is representative micrograph of Val129 variant and (C), is a representative micrograph of the mixture 1:1 of Met129 and Val129 variants. Aliquots of 3 μl were taken from samples containing amyloids as judged from ThT fluorescence, loaded onto carbon-coated, glow-discharged 400-mesh copper grids, blotted, negatively stained with 1% uranyl acetate, air dried and then viewed in a Zeiss (formerly Leo) Omega 912 electron microscope equipped with an in column charge-coupled device camera (2048 × 2048 pixels) from Proscan, Germany. The negative staining was performed on amyloid fibres derived from spontaneous amyloid reactions. (D, E) FTIR spectra and second derivatives, respectively, of the amyloid fibres produced from Met129 (*solid line*) and Val129 (*dashed line*) variants.

codon 129 on the kinetics of amyloid accumulation [10]. Instead, our findings indicate that the polymorphism at codon 129 of human PrP can exert its effect on the misfolding pathway that leads to amyloid accumulation only when PrP is in a partially disordered state. Furthermore, the relative ease with which the α-monomeric forms of PrP allelomorphs can transition to the amyloid state indicates that this process is relatively insensitive to the local, native conformational subtleties that might be conferred by the codon 129 polymorphism [10]. This is consistent with the finding that the solution structures and dynamic stabilities of recombinant human PrP are not affected by this polymorphism [13]. Since the effect of the polymorphism at codon 129 on the kinetics of amyloid formation seems to be dependent on the initial folding state of PrP, one could speculate that the residues involved in the initiation of the process, or even those that are participating structurally, may differ between pathway 3 and pathway 4 of amyloid formation (Fig. 1). Taken together our data strongly support a model, which postulates that: (i) the thermodynamic character of the native and denatured ensembles of PrP is variable and gradually changes with environment; (ii) the variable character of the native/denatured ensemble determines the diversity of misfolding pathways under different initial solvent conditions [20]. A direct implication of this would be that the amyloid formed under different pathways might differ slightly in their three-dimensional structure. Whether they also differ in their toxicity and infectivity, the question remains to be answered.

Taken together, our studies demonstrate the complexity and the profound effect that the polymorphic residue at position 129 can have on the misfolding pathways of human PrP. These data are in contrast with the observations made during the misfolding into oligomers, where the amount of oligomer seen with Met129 was much higher than with Val129 [9]. This further indicates that amyloid formation occurs through a pathway different from the one that leads to the oligomer, strengthening the previous finding that the β-sheet-rich oligomer is not on the kinetic pathway to amyloid formation and cannot be regarded as a substructure of the fibrillar form [8].

The observed differences in the kinetics of amyloid formation allow us to define precisely one of the regions involved in the rate-determining step of the aggregation process; the residue expressed at position 129 in this regard is critical. Our data show that the presence of a high β-sheet forming amino acid, such as valine [21,22] at position 129 accelerated the kinetics of amyloid formation and is consistent with molecular dynamics simulations [23]; providing a possible molecular mechanism for the faster nucleation rate of the Val129 variant relative to that of the Met129 variant. Residue 129 is within the first β-strand (residues 128–131) in human PrP. Riek et al. [24] proposed that this short β-sheet might be a 'nucleation site' for a conformational transition from PrP[C] to PrP[Sc] that could include the loops connecting the β-sheet to the first helix. Molecular dynamics simulations of Syrian hamster PrP[90–231] at neutral pH showed that when valine was present at position

129 instead of methionine additional β-strands may form involving residues 115–116 and 119–122. For the valine allelomorph, the percentage of molecules calculated to adopt this structure was 23% as opposed to 0% for the methionine allelomorph [23], but simulations also indicated that this does not affect thermodynamic stability, as has been found experimentally [11].

Using recombinant prion protein, we clearly demonstrate that the polymorphism at codon 129 in the *PrnP* gene impacts on the complexity of the misfolding pathways that lead to nonnative isoforms of prion protein. We have attempted to model the heterozygote genotype at this polymorphic site, by analysing abnormal folding pathway 4 (Fig. 1) in a 1:1 mixture of Met129 and Val129. The results showed intermediate behaviour with no obvious predominant effect of one variant over the other. The fact that we do not observe biphasic behaviour in the kinetics of amyloid formation seems to indicate that there is a certain degree of interaction between the two allelomorphs. This is supported by the compatibility of seeds in the cross-seeding experiments. Interestingly, this compatibility seems to be 100% if one judges only from the length of the lag phase in cross-seeding experiments. However, in terms of the rate of growth, the two allelomorphs seem to display partial compatibility, because the rate of growth is slower in cross-seeded reactions, relative to that in spontaneous self-seeded experiment. This indicates that the interactions between the two variants during the higher order folding processes are more complex than originally anticipated and warrants further investigation. The seeding experiments also show that the Val129 seeds are better seeds than the Met 129 seeds. We do not have a clear explanation for this behaviour. This may be attributed to the presence of more ends in the Val129 seeds that are available for polymerization or it could be due to subtle structural differences in the amyloid seeds that are intrinsic to the two variants.

We have used partially denaturing conditions in these in vitro conversion experiments. Although, these conditions seem far from physiological, they may approximate an environment leading to the formation of PrP^{Sc}. It is commonly accepted that conversion of PrP^{C} to PrP^{Sc} requires certain degree of unfolding of PrP^{C}. Several classes of molecules such as lipid membrane [25], salt [26] and some natural nucleic acids [27,28] were found to be capable of assisting the conversion of PrP^{C} into disease-related conformation by reducing thermodynamic stability of PrP^{C} and facilitating its unfolding. Chemical-induced denaturation used in our study, represent more generic way for shifting dynamic balance between native vs. unfolded states of PrP^{C}. Therefore, our experiments illustrate intrinsic propensity of human PrP to convert into amyloid forms and the dependence of this process on the polymorphism at codon 129.

The converse propensities of the Met129 and Val129 allelomorphs to fold into the β-oligomer and amyloid forms, respectively, is highly suggestive, given the effect of the polymorphism on disease susceptibility in vivo. We note that neither the β-oligomers nor the amyloids perfectly reflect the biophysical properties of PrP^{Sc}, the form traditionally associated with prion infectivity [16,29]. Specifically, the relative resistance of PrP^{Sc} to digestion with proteinase K is shown by the β-oligomer [9] but only partially by the amyloid [8], whereas the morphological appearance and dye-binding characteristics of PrP^{Sc} are reflected by the in vitro-formed amyloid

but not by the β-oligomer form. Our recent studies, however, demonstrated that amyloids produced under partially denaturing conditions are biochemically similar to the minor population of PrP^{Sc} identified in patient with sporadic CJD [20]. The formation of amyloids in vitro also displays a species barrier, one of the key features of prion replication [30]. Furthermore, fibrilar form of PrP has an epitope presentation similar to that of PrP^{Sc} [8].

The differences in the misfolding behaviour between Met129 and Val129 could form the basis to explain certain aspects of human TSEs, particularly sporadic CJDs, that are associated with codon 129 variations such as age at onset of the disease and incubation time [6,31–35]. Reports mainly suggested that the age at onset is lower and the disease duration longer in Val129 cases. This effect appears to be replicated in animal models of human disease: two out of three transgenic mice expressing human PrP Val129 showed a shorted incubation period [36] as compared with transgenic mice expressing human PrP Met129 [37] (and Jean Manson, personal communication) when challenged with a matching genotype inocula.

References

[1] Palmer, M.S., Dryden, A.J., Hughes, J.T. and Collinge, J. (1991) Homozygous prion protein genotype predisposes to sporadic Creutzfeldt–Jakob disease. Nature 352, 340–342.

[2] Brown, P., et al. (1994) Iatrogenic Creutzfeldt–Jakob disease: an example of the interplay between ancient genes and modern medicine. Neurology 44, 291–293.

[3] Collinge, J., Palmer, M.S. and Dryden, A.J. (1991) Genetic predisposition to iatrogenic Creutzfeldt–Jakob disease. Lancet 337, 1441–1442.

[4] Baker, H.E., Poulter, M., Crow, T.J., Frith, C.D., Lofthouse, R. and Ridley, R.M. (1991) Aminoacid polymorphism in human prion protein and age at death in inherited prion disease. Lancet 337, 1286.

[5] Cervenakova, L., Goldfarb, L.G., Garruto, R., Lee, H.S., Gajdusek, D.C. and Brown, P. (1998) Phenotype-genotype studies in kuru: implications for new variant Creutzfeldt–Jakob disease. Proc. Natl. Acad. Sci. USA 95, 13239–13241.

[6] Parchi, P., et al. (1999) Classification of sporadic Creutzfeldt–Jakob disease based on molecular and phenotypic analysis of 300 subjects. Ann. Neurol. 46, 224–233.

[7] Baskakov, I.V., Legname, G., Prusiner, S.B. and Cohen, F.E. (2001) Folding of prion protein to its native alpha-helical conformation is under kinetic control. J. Biol. Chem. 276, 19687–19690.

[8] Baskakov, I.V., Legname, G., Baldwin, M.A., Prusiner, S.B. and Cohen, F.E. (2002) Pathway complexity of prion protein assembly into amyloid. J. Biol. Chem. 277, 21140–21148.

[9] Tahiri-Alaoui, A., Gill, A.C., Disterer, P. and James, W. (2004) Methionine 129 variant of human prion protein oligomerizes more rapidly than the valine 129 variant: implications for disease susceptibility to CJD. J. Biol. Chem. 279, 31390–31397.

[10] Tahiri-Alaoui, A. and James, W. (2005) Rapid formation of amyloid from {alpha}-monomeric recombinant human PrP in vitro. Protein Sci. 14, 942–947.

[11] Liemann, S. and Glockshuber, R. (1999) Influence of amino acid substitutions related to inherited human prion diseases on the thermodynamic stability of the cellular prion protein. Biochemistry 38, 3258–3267.

[12] Riek, R., Wider, G., Billeter, M., Hornemann, S., Glockshuber, R. and Wuthrich, K. (1998) Prion protein NMR structure and familial human spongiform encephalopathies. Proc. Natl. Acad. Sci. USA 95, 11667–11672.

[13] Hosszu, L.L.P., et al. (2004) The residue 129 polymorphism in human prion protein does not confer susceptibility to Creutzfeldt–Jakob disease by altering the structure or global stability of PrPC. J. Biol. Chem. 279, 28515–28521.

[14] Baskakov, I.V., Legname, G., Gryczynski, Z. and Prusiner, S.B. (2004) The peculiar nature of unfolding of the human prion protein. Protein Sci. 13, 586–595.

[15] Legname, G., Baskakov, I.V., Nguyen, H.O., Riesner, D., Cohen, F.E., DeArmond, S.J. and Prusiner, S.B. (2004) Synthetic mammalian prions. Science 305, 673–676.

[16] Prusiner, S.B. (1982) Novel proteinaceous infectious particles cause scrapie. Science 216, 136–144.

[17] Wall, J., Schell, M., Murphy, C., Hrncic, R., Stevens, F.J. and Solomon, A. (1999) Thermodynamic instability of human lambda 6 light chains: correlation with fibrillogenicity. Biochemistry 38, 14101–14108.

[18] Tahiri-Alaoui, A., Bouchard, M., Zurdo, J. and James, W. (2003) Competing intrachain interactions regulate the formation of beta-sheet fibrils in bovine PrP peptides. Protein Sci. 12, 600–608.

[19] Bocharova, O.V., Breydo, L., Parfenov, A.S., Salnikov, V.V. and Baskakov, I.V. (2005) In vitro conversion of full-length mammalian prion protein produces amyloid form with physical properties of PrP(Sc). J. Mol. Biol. 346, 645–659.

[20] Bocharova, O.V., Breydo, L., Salnikov, V.V., Gill, A. and Baskakov, I.V. (2005) Synthetic prions generated in vitro are similar to a newly identified subpopulation of PrPSc from sporadic Creutzfeldt–Jakob disease. Protein Sci., in press.

[21] Fasman, G.D. (1989) Protein conformational prediction. Trends Biochem. Sci. 14, 295–299.

[22] Kim, C.A. and Berg, J.M. (1993) Thermodynamic beta-sheet propensities measured using a zinc-finger host peptide. Nature 362, 267–270.

[23] Santini, S., Claude, J.B., Audic, S. and Derreumaux, P. (2003) Impact of the tail and mutations G131V and M129V on prion protein flexibility. Proteins 51, 258–265.

[24] Riek, R., Hornemann, S., Wider, G., Billeter, M., Glockshuber, R. and Wuthrich, K. (1996) NMR structure of the mouse prion protein domain PrP (121–321). Nature 382, 180–182.

[25] Sanghera, N. and Pinheiro, T.J. (2002) Binding of prion protein to lipid membranes and implications for prion conversion. J. Mol. Biol. 315, 1241–1256.

[26] Nandi, P.K., Leclerc, E. and Marc, D. (2002) Unusual property of prion protein unfolding in neutral salt solution. Biochemistry 41, 11017–11024.

[27] Deleault, N.R., Lucassen, R.W. and Supattapone, S. (2003) RNA molecules stimulate prion protein conversion. Nature 425, 717–720.

[28] Nandi, P.K., Leclerc, E., Nicole, J.C. and Takahashi, M. (2002) DNA-induced partial unfolding of prion protein leads to its polymerisation to amyloid. J. Mol. Biol. 322, 153–161.

[29] Prusiner, S.B. (1991) Molecular biology of prion diseases. Science 252, 1515–1522.

[30] Baskakov, I.V. (2004) Autocatalytic conversion of recombinant prion proteins displays a species barrier. J. Biol. Chem. 279, 7671–7677.

[31] Windl, O., et al. (1996) Genetic basis of Creutzfeldt–Jakob disease in the United Kingdom: a systematic analysis of predisposing mutations and allelic variation in the PRNP gene. Hum. Genet. 98, 259–264.

[32] Laplanche, J.L., Delasnerie-Laupretre, N., Brandel, J.P., Chatelain, J., Beaudry, P., Alperovitch, A. and Launay, J.M. (1994) Molecular genetics of prion diseases in France. French research group on epidemiology of human spongiform encephalopathies. Neurology 44, 2347–2351.

[33] Schulz-Schaeffer, W.J., Giese, A., Windl, O. and Kretzschmar, H.A. (1996) Polymorphism at codon 129 of the prion protein gene determines cerebellar pathology in Creutzfeldt–Jakob disease. Clin. Neuropathol. 15, 353–357.

[34] Hauw, J.J., et al. (2000) Neuropathologic variants of sporadic Creutzfeldt–Jakob disease and codon 129 of PrP gene. Neurology 54, 1641–1646.

[35] Alperovitch, A., et al. (1999) Codon 129 prion protein genotype and sporadic Creutzfeldt–Jakob disease. Lancet 353, 1673–1674.

[36] Hill, A.F., Desbruslais, M., Joiner, S., Sidle, K.C., Gowland, I., Collinge, J., Doey, L.J. and Lantos, P. (1997) The same prion strain causes vCJD and BSE. Nature 389, 448–450, 526.

[37] Asante, E.A., et al. (2002) BSE prions propagate as either variant CJD-like or sporadic CJD-like prion strains in transgenic mice expressing human prion protein. EMBO J. 21, 6358–6366.